An Improved Worst-Case Response Time Analysis for AVB Traffic in Time-Sensitive Networks

1st Daniel Bujosa*, 2nd Julian Proenza†, 3rd Alessandro V. Papadopoulos*, 4th Thomas Nolte*, 5th Mohammad Ashjaei*
* *Mälardalen University*, Västerås, Sweden
daniel.bujosa.mateu@mdu.se, alessandro.papadopoulos@mdu.se, thomas.nolte@mdu.se, mohammad.ashjaei@mdu.se
† University of the Balearic Islands, Palma, Spain
julian.proenza@uib.es

***Abstract*—Time-Sensitive Networking (TSN) has become one of the most relevant communication networks in many application areas. Among several traffic classes supported by TSN networks, Audio-Video Bridging (AVB) traffic requires a Worst-Case Response Time Analysis (WCRTA) to ensure that AVB frames meet their time requirements. In this paper, we evaluate the existing WCRTAs that cover various features of TSN, including Scheduled Traffic (ST) interference and preemption. When considering the effect of the ST interference, we detect optimism problems in two of the existing WCRTAs, namely (i) the analysis based on the busy period calculation and (ii) the analysis based on the eligible interval. Therefore, we propose a new analysis including a new ST interference calculation that can extend the analysis based on the eligible interval approach. The new analysis covers the effect of the ST interference, the preemption by the ST traffic, and the multi-hop architecture. The resulting WCRTA, while safe, shows a significant improvement in terms of pessimism level compared to the existing analysis approaches relying on either the concept of busy period or the Network Calculus model.**

***Index Terms*—Worst-Case Response Time Analysis, Time Sensitive Networking, Audio-Video Bridging**

I. Introduction

Since its inception in 2012, Time-Sensitive Networking (TSN) has become one of the most relevant sets of standards for real-time communications. TSN provides Ethernet with various features, including precise clock synchronization, traffic flexibility, fault tolerance, and advanced network management. These characteristics make TSN relevant to several application areas, such as automation [1], automotive [2], and power distribution [3].

This paper focuses on two of TSN's most relevant features: its traffic flexibility and the real-time features it provides. Traffic flexibility allows mixing traffic with different characteristics and levels of real-time requirements on the same network. Traditionally, this has been addressed using several networks with different characteristics connected through gateways with limited inter-network connectivity. However, thanks to TSN, this separation is no longer necessary, as a single network can handle all types of traffic.

To achieve this, TSN defines three types of traffic: Scheduled Traffic (ST), Audio-Video Bridging Traffic (AVB), and Best-Effort Traffic (BE). ST can meet its requirements by construction as it is scheduled offline, and BE traffic has no Real-Time (RT) requirements. However, AVB traffic, despite being predictable, requires a Worst-Case Response Time Analysis (WCRTA) to determine whether it can meet its time requirements. WCRTAs can be optimistic, exact, or pessimistic. An optimistic analysis is unacceptable, as it may fail to meet the time requirements, potentially leading to catastrophic consequences in critical systems. In contrast, a pessimistic WCRTA, albeit safe, leads to wasted resources.

An exact WCRTA is preferred for analysis of any real-time systems; however, it is challenging to achieve and often impossible due to considering worst-case scenarios. To the authors' best knowledge, currently, there is no exact WCRTA for TSN's AVB traffic. Nevertheless, providing a WCRTA with as little pessimism as possible is essential when the exact analysis is unavailable. This paper proposes a WCRTA and shows that it is less pessimistic than the existing WCRTA for AVB traffic in literature.

Contributions: In this paper, we closely evaluate all the existing AVB WCRTAs that support AVB traffic analysis under ST interference with and without preemption of the ST since this is the most common configuration. Note that there are other WCRTAs that compute the Worst-Case Response Times (WCRT) of AVB traffic without ST interference or preemption, or WCRTAs of TSN, such as [4], that do not consider AVB traffic. Those works are considered limited in their capacity to support the TSN features, thus out of the scope of this evaluation. To the best of our knowledge, there are only two AVB WCRTAs in the literature that consider ST interference and preemption according to the standards, being an analysis based on the busy period calculation [5] and an analysis based on the Network Calculus model [6]. There is also a work based on the notion of eligible interval [7]–[9] that shows a significant improvement in terms of reducing pessimism compared to other analyses, but that is limited to a single TSN output port and that does not consider the ST interference. Further, there was an attempt to add the ST interference without preemption to the eligible interval analysis [10]. However, this paper shows that the approach presented in [10] contains a potential optimism in corner cases. The concrete contributions in this paper are as follows:

- First, we show that although the eligible interval approach for AVB traffic analysis presents less pessimism than the existing analysis approaches, the extended analysis presented in [10] to include the ST interference contains optimism in corner cases.

- Second, we show that the WCRTA based on the busy period calculation presented in [5] also contains optimism in calculating the ST interference, potentially making the analysis unsafe.
- Third, we propose a new calculation of the ST interference, solving the optimism problems in both analysis approaches.
- Fourth, we present a new WCRTA which extends the one based on the eligible interval approach [7]–[9] to consider ST interference with and without preemption and the effect of the multi-hop behavior instead of being limited to a single output port.
- Finally, we compare the three WCRTAs, i.e., the analysis based on the busy period calculation [5], the Network Calculus model [6], and the new analysis presented in this paper, for two different network sizes. We show that our analysis, while safe, significantly outperforms the other two by exhibiting much less pessimism, on average around 100% compared to the busy period [5] and 15% compared to the Network Calculus model [6].

Paper organization The paper is organized as follows. Section II introduces the concepts and features of TSN. Section III reviews the related works, while Section IV defines the system model. Section V summarizes the WCRTA based on the eligible interval, and Section VI extends it by adding the proposed ST interference calculation and the multi-hop behavior effect. Section VII presents the experimental setup, while Section VIII shows the results. Finally, Section IX concludes the paper.

II. Recap on TSN Traffic Shapers

In TSN, communication between end-stations relies on transmitting Ethernet frames through Ethernet links and TSN switches. TSN switches and end-stations output ports have up to 8 First-In-First-Out (FIFO) queues. Each queue corresponds to one of the 8 priorities available in TSN. Each of these queues can apply different traffic shapers. Depending on the queue configuration, it can handle one of the three types of TSN traffic (ST, AVB, or BE). As many queues as needed from the 8 available priorities can be allocated to each type of traffic, resulting in more than one class in AVB and BE.

Fig. 1 shows an example of a simplified 4-queue output port consisting of an ST queue, two AVB queues (class A and B), and a BE queue. The following sections will explain each TSN traffic shaper and how they are configured.

A. Time-Aware Shaper

ST is pre-scheduled offline to ensure precise transmission with high accuracy and zero jitter. To meet the determinism requirements of ST and prevent inter-frame interference, TSN employs the Time-Aware Shaper (TAS) mechanism. TAS operates by isolating queues eligible for transmission and assigning to each queue a gate that can be toggled between open and closed states. The state of the gate is determined by the Gate Control List (GCL), specifying, at the nanosecond level, the duration for which a gate should be open or closed in a cyclically repeating list. The cycle length is determined by the hyper-period of the ST frames transmitted through

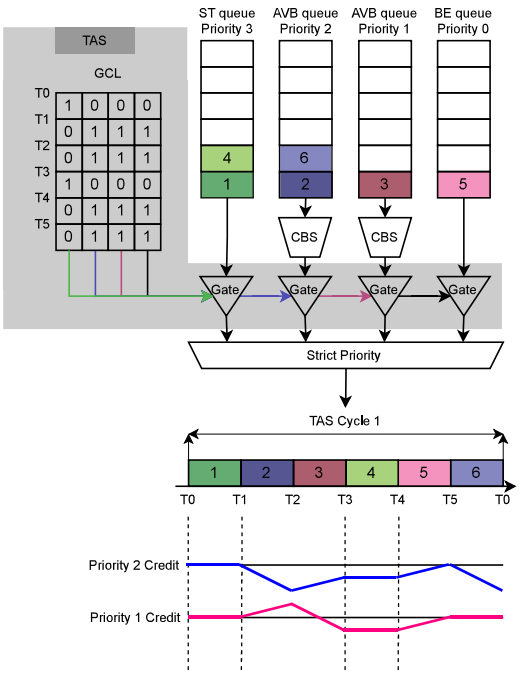

Fig. 1. Example of TSN output port.

the corresponding output port. This is a limitation of the ST traffic due to the potential for certain period combinations to cause an explosion in the length of the GCL, underscoring the significance of AVB traffic. An open gate allows traffic transmission from the queue, whereas a closed gate prevents frames from being transmitted. The open gate period is a *transmission window*. For a scheduled transmission of an ST frame at a designated time, the frame must reside in the assigned queue, and the gate of that queue must remain closed until the scheduled transmission time. Before the transmission window starts, all gates of other queues are closed to prevent interference. This time when all gates are closed is called *guard band*. Then, the ST queue gate opens precisely at the scheduled time for the transmission of the ST frame. This mechanism is referred to as the HOLD/RELEASE mechanism in the standards.

Additionally, TSN can be configured so that ST traffic can preempt the non-scheduled traffic (AVB and BE traffic), commonly known as non-ST traffic. That is, the transmission of the non-ST frame halts temporarily and resumes after the ST frame completes its transmission. The guard band size varies based on whether TSN is configured with or without preemption. With preemption, the guard band needs to exceed the minimum preemptible message size (124 Bytes). Whereas, without preemption, the guard band must be greater than the maximum size of a TSN frame, which is 1518 Bytes. Alternatively, not adding guard bands would result in jitter for the ST equivalent to the transmission time.

Fig. 1 shows an example with two ST frames (1 and 4). This example does not include guard bands or preemption for simplicity. According to the GCL, these frames are scheduled

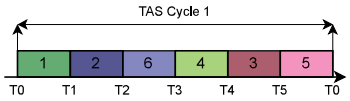

Fig. 2. TSN output port transmission considering only TAS and strict priority.

to be sent at times T0 and T3, respectively. Thus, as depicted in the figure, at time T0, the ST gate is open, and all other gates are closed, enabling the transmission of frame 1 without interferences. Then, between T1 and T3, the ST gate is closed, and the other gates are open, enabling the transmission of the non-ST traffic. At T3, the ST gate is reopened, and the other gates are closed to allow the transmission of frame 4 without interference. Finally, the ST gate is closed, and the non-ST gates are opened to enable the transmission of the remaining non-ST frames.

B. Credit-Based Shaper

While ST is transmitted according to a fixed schedule with zero jitter, its reliance on off-line scheduling considerably reduces its effectiveness and efficiency in handling other traffic types, such as event-triggered traffic. Additionally, the cost of obtaining a schedule substantially increases with the number of frames to be scheduled and may not always be affordable or even feasible. This is where non-ST traffic comes into play. Non-ST can be transmitted when its gate is open, i.e., when no ST frames are transmitted.

Without additional mechanisms, non-ST traffic would be subject to arbitration through strict priority, severely impacting the quality of service for lower-priority queues and significantly impairing their real-time response guarantees. Fig. 2 illustrates the transmission outcome under arbitration solely by TAS and strict priority. Frames from lower-priority queues experience delayed transmission, with the delay increasing as the queue's priority decreases. In the most extreme scenario, a high-priority queue may indefinitely interfere with low-priority queues, causing an infinite delay in their transmissions.

TSN incorporates a Credit-Based Shaper (CBS) mechanism to overcome this limitation. The traffic assigned to queues implementing CBS is the AVB traffic, while the lowest-priority queue with no CBS is the BE traffic. CBS limits the maximum percentage of bandwidth a queue can utilize, ensuring a minimum bandwidth allocation for lower-priority queues. In CBS, credit is assigned to each AVB queue. The credit is progressively replenished when an AVB frame awaits to be transmitted or the credit is negative and is consumed when a frame is being sent. The replenishment and consumption rates of the credit are denoted by the terms *idleSlope* and *sendSlope*, respectively. A queue is eligible for transmission only if its credit is zero or a positive value. According to the standard, the credit of a queue freezes if its gate is closed.

Additionally to the ST queue, the example in Fig. 1 includes two AVB queues and one BE queue. Two frames (2 and 6) are assigned to the higher-priority AVB queue, while the lower-priority AVB queue and the BE queue present a single frame (frames 3 and 5, respectively). At time T1, following the transmission of the ST frame, both AVB queues become eligible for transmission. Consequently, the strict priority mechanism selects the priority 2 AVB queue, leading to the transmission of frame 2. While the frame is transmitted, its credit is consumed. At the same time, the credit of the lower-priority AVB queue is replenished as it awaits transmission.

Moving to T2, the higher-priority AVB queue, having negative credit, becomes ineligible for transmission. Subsequently, the lower-priority AVB queue is chosen, resulting in the transmission of frame 3. Remarkably, this occurs even when a higher-priority non-ST frame (frame 6) awaits the transmission. Similarly to T1, priority 1 credit is consumed during the transmission of frame 3, while the higher-priority AVB credit is replenished.

At T3, another ST frame is transmitted, and the gates of the AVB queues close, causing their credit to freeze. By T4, the credit of both AVB queues is negative, prompting the BE queue to be selected for transmission. This choice occurs even though a higher-priority AVB frame awaits the transmission. Finally, at T5, the credit of the higher-priority AVB queue becomes zero, allowing for the transmission of the last frame (frame 6). Note that BE has no timing requirement and can only be transmitted when its gate is open, and no other higher-priority frame is eligible to be transmitted.

III. Related Work

Since the introduction of the AVB standard in 2011, numerous papers have delved into the challenge of analyzing its WCRT. However, almost all of them can be categorized into three distinct approaches, including busy period analysis, Network Calculus model, and eligible interval analysis.

The busy period analysis relies on finding the critical instant producing the WCRT. Diemer et al. [11] introduced one of the first AVB WCRTAs based on busy period analysis. Nevertheless, it was constrained to a single output port and a single AVB queue and did not account for ST interference. Subsequently, the work in [12] extended the previous work to include the analysis of two AVB queues (class A and class B). However, the consideration of ST was still omitted and confined to only one output port. Finally, in the work by Lo Bello et al. [5], one of the last AVB WCRTA based on busy period analysis is introduced. Apart from considering interference with other AVB classes, this paper also incorporates the impact of ST interference with and without preemption of non-ST traffic and the blocking of lower-priority frames. Moreover, it includes a multi-hop calculation, i.e., it is not constrained to a single output port. However, it is important to note that the paper is limited to two AVB classes (Class A and B). Furthermore, this paper shows that the analysis contains optimism in the ST interference calculation.

The second approach leverages Network Calculus, a theoretical framework designed for the performance analysis of communication networks. Network Calculus allows for calculating the maximum delay each frame may experience, i.e., its WCRT. Zhao et al. [6], [13] introduce the WCRTA of AVB implemented using Network Calculus. This method enables the calculation of the WCRT from the transmitter to the receiver for multiple AVB queues considering ST interference with and without preemption of non-ST traffic. However,

limitations in Network Calculus arise when dealing with loop networks that involve circular dependencies. Furthermore, this approach allocates the same bandwidth for an AVB class on all links, reducing flexibility in configuration and potentially leading to situations where more bandwidth than necessary is reserved. This solution, along with the one presented in [5], is unique in providing WCRT from the transmitter to the receiver, encompassing ST interference and preemption of non-ST traffic by the ST. However, they have never been compared as they were developed in parallel and published at almost the same time. As part of the experiments in this paper, we also compare these two analysis approaches. While other WCRTAs based on Network Calculus exist, they do not meet the criteria for inclusion in this paper. For instance, [14] introduces a WCRTA based on Network Calculus designed for a highly specific setup featuring a single transmission window for each traffic type. Moreover, it restricts the AVB Class A and B gates from being opened simultaneously, significantly constraining the arbitration capabilities of CBS.

The third and final approach defines the time interval in which each frame can be eligible to be transmitted (*eligible interval*). The WCRT for a frame can be calculated by analyzing the maximum interference it may encounter throughout its eligible interval. Bordoloi et al. [15] introduced one of the earliest versions of the WCRTA, although the term had not yet been established. In the work by Cao et al. [7]–[9], the authors extend Bordoloi et al. [15] AVB's WCRTA and introduce the term eligible interval. They demonstrate that the maximum delay an AVB frame can experience, i.e., its WCRT, depends solely on the maximum credit attainable by its AVB class, while this maximum credit is bounded and can be calculated. This analysis makes WCRTs notably less pessimistic than those based on the busy period analysis or the Network Calculus model. Moreover, this analysis can be applied to any number of AVB classes. However, this analysis does not consider the interference caused by ST and is limited to a single output port. Maxim et al. [10] extended the AVB's WCRTA based on the eligible interval to incorporate ST interference, yet without preemption. However, as we will see later in this paper, the solution contains optimism when considering the ST interference.

As reviewed above, the existing analysis approaches either exhibit limitations or contain optimism. Therefore, this paper addresses such limitations and proposes a new ST interference calculation on the AVB traffic on multi-hop networks that results to a significantly less pessimistic analysis compared to the state-of-the-art analysis solutions.

IV. System Model

A. Network model

In the network topology, unidirectional connections between any end-station and any TSN switch and between two TSN switches are done through *link*s denoted by l. The TSN ports are considered full-duplex, i.e., the inputs and outputs are isolated. Therefore, reception and transmission do not interfere on the same physical port. This means that for each physical port, there are two links, one for sending and one for receiving. Moreover, the time that elapses from the reception of a frame through a TSN switch port until it is inserted into the queue at the output port is specific to each TSN switch and is denoted by ϵ. The link delay due to the wire and its physical characteristics is assumed to be negligible for the analysis, and the total network bandwidth is denoted by BW and is the same in all network links. Finally, for AVB traffic of priority X, on a link l, the credit replenishment rate (idleSlope) is denoted by $\alpha^{+}_{X,l}$, the credit consumption rate (sendSlope) is indicated as $\alpha^{-}_{X,l}$, and the credit value is denoted by $CR_{X,l}$.

B. Traffic model

In this paper, we use the real-time periodic model for all traffic. This model defines frames as a sequence of frame instances that share common characteristics, such as source and destination addresses, periods, deadlines, etc. In this sense, a set of N frames is characterized as follows:

$$\Gamma = \{m_i(C_i, T_i, D_i, P_i, \mathcal{L}_i, \mathcal{O}_i) | i = 1, \ldots, N\} \qquad (1)$$

In this model, C_i represents the transmission time of a m_i frame, which depends on the frame size and network bandwidth. Moreover, the header of each Ethernet frame is included in the frame transmission time C_i, and the header transmission time is denoted by v. This value will be considered constant and independent of the frame class. Regarding the ST, the guard band is also included in C_i when necessary. Note that when multiple ST frames are transmitted consecutively, only the first frame requires a guard band. Moreover, T_i and D_i denote the period and relative deadline of the frame. We also assume a constrained deadline model, i.e., $D_i \leq T_i$. Note that the AVB traffic classes can be initiated periodically or sporadically. In the case of sporadic transmissions, T_i represents the minimum inter-arrival time, i.e., the minimum time between initiations. The traffic priority of a frame is denoted by $P_i \in \mathbb{P}$. The priority level is the highest for the ST, the lowest for BE, and all middle ones are for AVB. In this regard, ST priority is denoted by P_{ST}, BE priority is denoted by P_{BE}, and AVB priorities are denoted by $(\{P \in \mathbb{P} \mid P_{ST} > P > P_{BE}\})$. Moreover, $\mathbb{L}$ and $\mathbb{H}$ are the sets of non-ST frames with lower and higher priority than m_i, respectively. As a frame may cross several links, the set of n links that m_i traverses is specified by $\mathcal{L}_i = \{l_1, \ldots, l_n\}$.

Offsets are used to accommodate ST frames in the transmission schedule. The offset for each ST frame is defined per link, and the set of offsets for all links that m_i crosses is specified by $\mathcal{O}_i$, e.g., $\mathcal{O}_i = \{O^l_i\}$. We assume that the offsets are given, as scheduling optimization for ST frames is out of the scope of this paper. Other works have already addressed this topic, such as [16]. Note that no offset is defined for AVB frames; hence, for AVB frames, $\mathcal{O}_i$ is an empty set, i.e., $\mathcal{O}_i = \{\emptyset\}$.

In this model, we consider the TSN configuration in which ST traffic can preempt the non-ST traffic. This implies that certain frames might experience interruptions during their transmission, only to be resumed later. Secondly, ST frames arriving at a switch will stay in the output queue until their transmission window becomes active. Specifically, the traffic classes can be classified as *express* or *preemptable*. Our system

model considers the ST frames to be express, whereas all the other classes are preemptable. This means that the guard band can be sized as 124 Bytes since this is the non-preemptable segment of any non-ST frame, i.e., is the maximum time a preemptable frame (non-ST frame) can block an express frame (ST frame). This is the most common TSN configuration when all traffic types are considered.

Finally, when an ST frame preempts a non-ST frame, it is resumed after preemption but with a new header. This means that when a frame is preempted and is split into two segments, the second segment also gets a header, i.e., two headers should be accounted for. This affects the analysis for AVB traffic, which will be discussed later in Section VI.

V. Worst-Case Response Time Analysis

This section will give a detailed overview of the WCRTA based on the eligible interval [7]–[9]. As mentioned above, this WCRTA only considers interference from AVB frames of higher and same priority, as well as lower-priority frames blocking, including lower-priority AVB traffic and BE traffic. In addition, it considers only one output port. Therefore, in the next section, we will extend this analysis to consider interference with ST and the contribution of multi-hop behavior.

A. WCRTA overview

We will begin by introducing each of the sources of delay that an AVB frame m_i in link l may experience according to the WCRTA based on the eligible interval. First, given that all queues in TSN are FIFO, a frame's transmission depends on the preceding frames within the same queue. Therefore, the first source of delay comes from interference with the same-priority traffic, denoted by SPI_i^l. Secondly, higher-priority AVB classes can also interfere with lower-priority AVB traffic, denoted by HPI_i^l, albeit to a restricted extent, thanks to the CBS mechanism. Finally, since AVB Classes are not preemptive, if frames from the lower-priority classes are being transmitted, an AVB frame should wait for its entire transmission. This entails a blocking by the lower-priority traffic, denoted by LPI_i^l. Summarizing, both the higher- and same-priority AVB traffic, as well as the lower-priority traffic (lower-priority AVB traffic and BE traffic), must be considered to compute the WCRT of any AVB frames, i.e., for a frame m_i crossing link l, the $WCRT_i^l$ considering only non-ST interference is:

$$WCRT_i^l = HPI_i^l + SPI_i^l + LPI_i^l + C_i \tag{2}$$

In the following subsections, we present the worst-case scenarios for each of the above components that build the WCRT for an AVB frame m_i on link l.

B. Same Priority Interference

According to [7]–[9], the delay experienced by an AVB frame m_i in link l interfered solely by its same-priority traffic, i.e., $sp(m_i) = \{m_j | P_j = P_i, j \neq i\}$, is calculated as a basic FIFO schedule. However, due to CBS behavior, not only the interference corresponding to the transmission of each same-priority frame C_j must be considered, but also the time required to recover the credit consumed by such interfering frame should be considered. This occurs because when only same-priority interference is considered, the credit can only increase when negative. The credit cannot become positive in this case because no other traffic is interfering with or blocking the traffic with the same priority as the frame under analysis. This behavior follows the CBS mechanism. As a result, the maximum attainable credit is zero, i.e., the credit decreases when a same-priority frame is being transmitted and increases only until zero. Consequently, the interference of every same-priority frame m_j will drop the credit to a negative value equal to $C_j \times \alpha^-_{P_i,l}$. Since an AVB class cannot transmit unless its credit is positive or zero, the next same-priority frame in the queue has to wait for the credit to recover. The recover time is calculated by $C_j \times \frac{\alpha^-_{P_i,l}}{\alpha^+_{P_i,l}}$. Therefore, the interference is the summation of the interfering frame transmission time and the time to recover the credit. In the worst case, frame m_i is interfered by all the same-priority frames. Since we consider the deadline-constrained model, each same-priority frame in the FIFO queue can interfere with m_i only once if all frames meet their deadlines, as it is already discussed in the Controller Area Network (CAN) domain [17]. In this context, as is common with most deadline-constrained analyses, the result lacks reliability if the WCRT exceeds the deadline of at least one same-priority frame. Therefore, the interference of the same-priority frames on m_i belonging to the class P_i on link l is calculated as in Eq. (3).

$$SPI_i^l = \sum_{\substack{\forall m_j \in sp(m_i), i \neq j \\ \wedge l \in \mathcal{L}_j}} C_j \times \left(1 + \frac{\alpha^-_{P_i,l}}{\alpha^+_{P_i,l}}\right) \tag{3}$$

C. Higher-Priority AVB Interference and Lower-Priority Blocking

Although the higher-priority AVB interference and the lower-priority blocking are two different contributions, the authors in [9] demonstrated that these delay contributions correspond to the time needed to reach the maximum credit CR^{max} achievable by the AVB class of the frame under analysis m_i with priority P_i, i.e.

$$HPI_i^l + LPI_i^l = \frac{CR^{max}_{P_i,l}}{\alpha^+_{P_i,l}} \tag{4}$$

The authors also proved that $CR^{max}_{P_i,l}$, and therefore the $HPI_i^l + LPI_i^l$, is bounded as long as the sum of the bandwidth allocated to P_i and all the higher priority queues $\mathbb{H} = \{H \in \mathbb{P} \mid ST > H > P_i\}$ does not exceed the available bandwidth. i.e.:

$$\sum_{\forall P \in \mathbb{H} \cup P_i} \alpha^+_{P,l} \leqslant BW. \tag{5}$$

Under these conditions, the non-ST interference $HPI_i^l + LPI_i^l$ that a frame can experience is computed as below:

$$\begin{aligned} HPI_i^l + LPI_i^l &= \frac{CR^{max}_{P_i,l}}{\alpha^+_{P_i,l}} \\ &= C^{max}_{\mathbb{L},l} \times \left(1 + \frac{\alpha^+_{\mathbb{H},l}}{\alpha^-_{\mathbb{H},l}}\right) - \frac{CR^{min}_{\mathbb{H},l}}{\alpha^-_{\mathbb{H},l}} \end{aligned} \tag{6}$$

where $C^{max}_{\mathbb{L},l}$ is the size of the largest frame of all lower priority queues $\mathbb{L} = \{L \in \mathbb{P} \mid L < P_i\}$ and $CR^{min}_{\mathbb{H},l}$ is the minimum value that the joint credit of the highest priority queues can reach in link l. The latter value is calculated recursively as follows:

$$CR^{min}_{\mathbb{H}=\{H_1,\ldots,H_n\},l} = -\max(\alpha^{-}_{\mathbb{H},l} \times C^{max}_{H_1,l} - CR^{min}_{\mathbb{H}-H_1,l}, \ldots, \alpha^{-}_{\mathbb{H},l} \times C^{max}_{H_n,l} - CR^{min}_{\mathbb{H}-H_n,l}) \quad (7)$$

VI. Proposed ST Interference

This section outlines the primary contributions of our work. Firstly, we introduce a novel method for calculating ST interference. Secondly, we incorporate this calculation along with the delay associated with multi-hop behavior into the WCRTA based on the eligible interval.

A. ST Interference

Excluding the WCRTAs based on the Network Calculus model, there have been 2 main attempts to calculate the ST interference on the AVB frames.

The work in [10] introduced a modified version of the WCRTA based on the eligible interval for a single link, considering the presence of ST. However, this study did not establish the independence of the eligible interval from ST interference. Additionally, the paper suggested that the maximum ST interference an AVB frame might experience is limited to all ST transmissions in a TAS Cycle.

$$STI^l = \sum_{\forall j \in ST} C_j \quad (8)$$

Nonetheless, this viewpoint is optimistic as nothing prevents an AVB frame from being interfered by more than one TAS cycle, as we see below.

Optimism in ST interference calculation in [10]: Consider an output port with a single ST frame of C = 1 tu and T = 2 tu and two AVB frames (frames 2 and 3) of C = 1 tu and T = 4 tu. Note that while the analysis considers two AVB queues (Class A and B), a single AVB queue example suffices to illustrate the optimism problem in the analysis. Regarding the GCL, i.e., the TAS cycle, it will be 2 tu long because there is only one ST frame with T=2 tu (TAS cycle equals the hyper-period of all ST frames). In each TAS cycle, 1 tu is allocated to the ST frame transmission and one is free for an AVB frame transmission. In this example, since there is only one AVB queue, we can assume that the credit is 100% for this queue, i.e., $\alpha^{+}_{P_0} = 1$. Therefore, no credit is consumed, hence there is no need to wait for its replenishment. According to [10], the delay experienced by either of the two AVB frames would be:

$$WCRT^l_i = STI^l_i + SPI^l_i + C_i = 1 + 1 + 1 = 3tu \quad (9)$$

However, as shown in Fig. 3, frame 3 experiences a WCRT:

$$WCRT^l_3 = STI^l_3 + SPI^l_3 + C_3 = 2 + 1 + 1 = 4tu \quad (10)$$

The analysis in [10] considers the ST interference in this example 1 tu, while it should be 2 tu, thus imposing optimism.

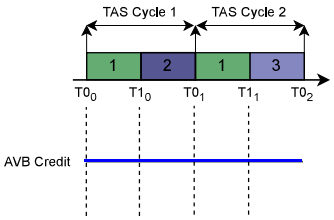

Fig. 3. Example of optimism on ST interference with AVB traffic.

Besides the work introduced above, the work in [5] proposed that the ST interference calculation consists of identifying the critical instant that generates the maximum interference on the AVB frame under analysis which in turn creates the maximum WCRT.

As proven in their work, the starting time of every ST transmission window in the hyper-period is a critical instant candidate. Since each link has a distinct hyper-period of length Ω_l, and given that the hyper-period of a set of frames is determined by the least common multiple of their periods, the instants to consider for the ST interference of $m_j \in ST$ on link $l \in \mathcal{L}_j$ are:

$$I^l_j = \{(k-1)T_j + O^l_j \ : k = 1, \ldots, n \ , \ n = \frac{\Omega_l}{T_j}\} \quad (11)$$

After obtaining all potential critical instants across the hyper-period on link l, it is necessary to calculate the phase difference between each ST frame $m_j \in ST$ and each potential critical instant $I^l_c[k]$. These phase differences are the offsets that the different ST frames would have if the start of the hyper-period were at the critical instant candidate. For more information and the proofs, the reader is referred to [18].

$$\Phi^l_{jc[k]} = (O^l_j - I^l_c[k]) \bmod T_j \quad (12)$$

Finally, for each critical instant candidate $I^l_c[k]$, the amount of ST interference that an AVB frame would experience over time t is :

$$W^l_{c[k]}(t) = \sum_{\forall j \in ST \ \wedge l \in \mathcal{L}_j} \left(\left\lfloor \frac{\Phi^l_{jc[k]}}{T_j} \right\rfloor + \left\lceil \frac{t - \Phi^l_{jc[k]}}{T_j} \right\rceil \right) C_j \quad (13)$$

Additionally, AVB traffic will be preempted for each ST frame interfering, resulting in additional headers being transmitted. Therefore, for each preemption by an ST frame, an additional interference by the header size v should be considered as shown in Eq. (14).

$$V^l_{c[k]}(t) = \sum_{\forall j \in ST \ \wedge l \in \mathcal{L}_j} \left(\left\lfloor \frac{\Phi^l_{jc[k]}}{T_j} \right\rfloor + \left\lceil \frac{t - \Phi^l_{jc[k]}}{T_j} \right\rceil \right) v \quad (14)$$

Therefore, the maximum ST interference an AVB frame m_i can experience in link l at instant $I^l_c[k]$ over a time t is computed in Eq. (15), which is the summation of interference

by ST and the extra headers due to preemption.

$$STI^{l}_{c[k]}(t) = W^{l}_{c[k]}(t) + V^{l}_{c[k]}(t) = \sum_{\forall j \in ST \wedge l \in \mathcal{L}_j} \left(\left\lfloor \frac{\Phi^{l}_{jc[k]}}{T_j} \right\rfloor + \left\lceil \frac{t - \Phi^{l}_{jc[k]}}{T_j} \right\rceil \right) (C_j + v) \quad (15)$$

In this way, the response time of an AVB frame enqueued in the output port of link l in the critical instant candidate $c[k]$, denoted by $STRT^{l,(x)}_{i,c[k]}$, is calculated iteratively as follows.

$$STRT^{l,(x)}_{i,c[k]} = STI^{l}_{c[k]} \left(STRT^{l,(x-1)}_{i,c[k]} \right) + HPI^{l}_{i} + SPI^{l}_{i} + LPI^{l}_{i} + C_i. \quad (16)$$

The iteration starts from $STRT^{l,(0)}_{i,c[k]} = HPI^{l}_{i} + SPI^{l}_{i} + LPI^{l}_{i} + C_i$ and terminates when $STRT^{l,(x)}_{i,c[k]} = STRT^{l,(x-1)}_{i,c[k]}$.

The worst-case response time of the frame m_i in link l is denoted by $STWCRT^{l}_{i}$. This interference is determined by selecting the largest response time among all critical instant candidates, i.e., the interference for all critical instant candidates should be evaluated and the maximum should be selected as follows:

$$STWCRT^{l}_{i} = \max_{\forall m_c, \forall k} \{ STRT^{l}_{i,c[k]} \} \quad (17)$$

Optimism in ST interference calculation in [5]: While this solution does cover all potential interferences, unlike the one proposed in [10], it remains optimistic about the magnitude of these interferences which potentially can make the analysis unsafe in corner cases. We show this optimism in a counter-example as follows.

Fig. 4(c) illustrates the response time of an AVB frame m_i with C_i = 4 tu, interfered by another same-priority frame with the same frame size (C_j = 4 tu) and an ST frame with C_k = 5 tu, taking into account the guard band and frame size. Moreover, for the sake of simplicity, both credit slopes $\alpha^{+}_{P_i,l}$ and $\alpha^{-}_{P_i,l}$ are assigned a value of 0.5, and the header is assigned a value of 1 tu. In this scenario, the analysis by [5] - Eqs. (15), (16), and (17) - yields the following calculated value:

$$STWCRT^{l}_{i} = STI^{l}_{i} + SPI^{l}_{i} + C_i = 5 + 1 + 8 + 4 = 18tu \quad (18)$$

However, as depicted in the diagram, m_i experiences a delay of 4 tu due to the transmission of the same-priority frame, another 5 tu for the transmission of the ST frame along with the guard band, an additional 1 tu for the header required to resume the transmission of the same-priority frame, 5 tu to recover the consumed credit, and finally, 4 tu of C_i, resulting in a WCRT of 19 tu, proving the optimism in the analysis. Although some analyses, such as [19], consider that the credit freeze during the transmission of the bytes related to the preemption overhead, this only applies to the end-of-frames transmitted during the guard band. That is because during the guard band, the gates of the AVB queues are closed and, according to the most common TSN implementation, the credit of a queue is frozen while its gate is closed. However, the additional headers are transmitted once the AVB gate is reopened so their credit is consumed.

The main issue with these ST interference calculations is the absence of analysis concerning their interaction with other types of traffic, i.e., considering the ST interference as an independent term in the analysis. In the following subsections, we will delve into the interactions between ST and other types of traffic. Initially, we will focus on same-priority traffic before integrating higher- and lower-priority traffic into the analysis.

B. ST and Same-Priority Interference Interaction

We show the effect of ST preemption with same-priority interference via a lemma. In this subsection, we consider the interference of ST when there is interaction with only same-priority interference.

Lemma 1: The WCRT of m_i in link l in the presence of ST and only same-priority interference with ST preemption in the critical instant candidate $I^{l}_{c}[k]$ is calculated as follows:

$$STRT^{l,(x)}_{i,c[k]} = W^{l}_{c[k]} \left(STRT^{l,(x-1)}_{i,c[k]} \right) + V^{l}_{c[k]} \left(STRT^{l,(x-1)}_{i,c[k]} \right) \times \left(1 + \frac{\alpha^{-}_{P_i,l}}{\alpha^{+}_{P_i,l}} \right) + SPI^{l}_{i} + C_i \quad (19)$$

Proof 1: In this scenario, there are only three possible cases of ST interference as follows: (i) when the ST interference occurs during credit recovery, thus not preempting any frame (as shown in Fig. 4(a)); (ii) when the ST interference occurs during the transmission of the frame under analysis (as shown in Fig. 4(b)); and (iii) when the ST interference happens while a frame of the same priority as the one under analysis is being transmitted (as shown in Fig. 4(c)).

As depicted in Fig. 4(a), the scenario without preemption produces the shortest response time. This is because this type of ST interference does not introduce any extra delay beyond the time associated with the transmission window of the ST frame, i.e., $W^{l}_{c[k]}(t)$ in Eq. (13). Conversely, the case shown in Fig. 4(b) is the scenario considered in [5]. In this scenario, the ST frame preempts the frame under analysis. In this case, alongside the contribution related to the transmission window of the ST frame $W^{l}_{c[k]}(t)$, it is necessary to add the delay corresponding to the header required to resume the transmission of the frame under analysis, i.e., $V^{l}_{c[k]}(t)$ in Eq. (14). This result corresponds to the one shown in Eqs. (15), (16), and (17). Finally, Fig. 4(c) shows the case in which the ST frame preempts frames of the same priority as the frame under analysis. In this case, additionally to the contribution related to the transmission window of the ST frame $W^{l}_{c[k]}(t)$, and the delay corresponding to the header required to resume the transmission of the same-priority frame, $V^{l}_{c[k]}(t)$, it is necessary to add the delay corresponding to the recovery of the credit consumed during the transmission of the extra header.

The third case, also shown in Fig. 4(c), results in the worst-case situation that can occur to the frame under analysis, which was not considered in the previous work [5]. When ST preempts the same-priority traffic, the transmission time of frames of the same priority is extended by v for each preemption, i.e., $V^{l}_{c[k]}(t)$. The credit consumed during the transmission of

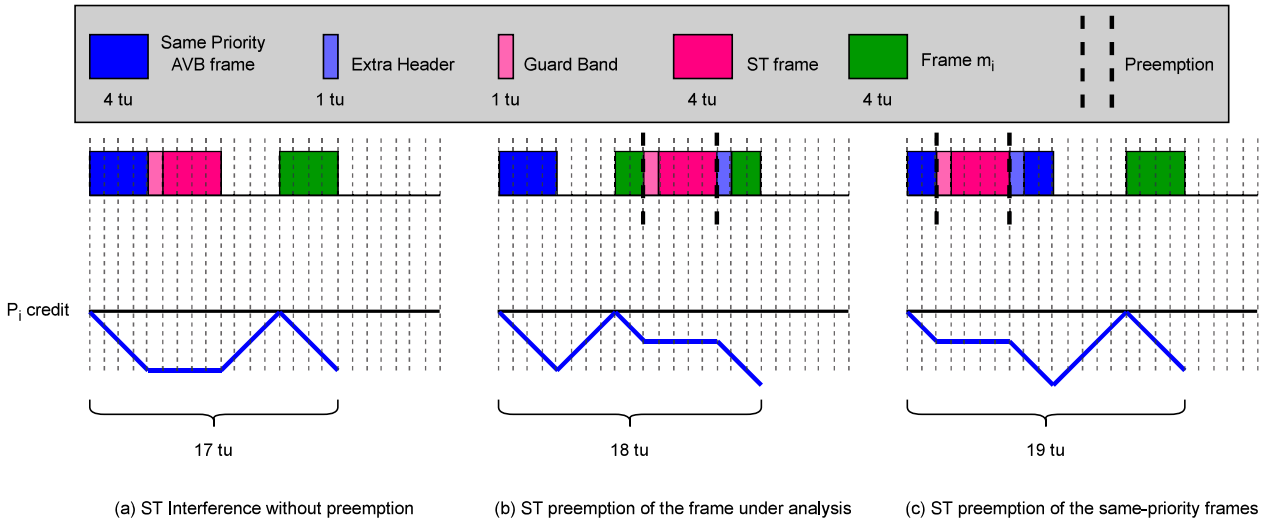

Fig. 4. Example of worst-case ST preemption.

$V^l_{c[k]}(t)$ is $V^l_{c[k]}(t) \times \alpha^-_{P_i,l}$. As explained in Section V-B, all consumed credit must be recovered to allow the transmission of the same-priority traffic. The time required to recover the credit consumed by $V^l_{c[k]}(t)$ is calculated by $V^l_{c[k]}(t) \times \frac{\alpha^-_{P_i,l}}{\alpha^+_{P_i,l}}$ which by adding $V^l_{c[k]}(t)$ we obtain $V^l_{c[k]}(t) \times \left(1 + \frac{\alpha^-_{P_i,l}}{\alpha^+_{P_i,l}}\right)$. Therefore, the term for calculating the contribution of multiple headers due to the ST preemption should be modified, proving the lemma.

C. ST and Non-ST Interference Interactions

In this subsection, we consider the interference of ST when there is interaction with all non-ST frame interference, including the same-priority interference.

Lemma 2: The WCRT of m_i in link l in the presence of ST interference, higher-priority AVB traffic interference, lower-priority blocking, and same-priority interference in the critical instant candidate $I^l_c[k]$ is calculated as follows:

$$\begin{aligned} STRT^{l,(x)}_{i,c[k]} = \\ & W^l_{c[k]}\left(STRT^{l,(x-1)}_{i,c[k]}\right) \\ & + V^l_{c[k]}\left(STRT^{l,(x-1)}_{i,c[k]}\right) \times \left(1 + \max\left(\frac{\alpha^-_{P_i,l}}{\alpha^+_{P_i,l}}, \frac{\alpha^+_{\mathbb{H},l}}{\alpha^-_{\mathbb{H},l}}\right)\right) \\ & + HPI^l_i + LPI^l_i + SPI^l_i + C_i \end{aligned} \tag{20}$$

Proof 2: Alongside the three cases of ST interference in the interaction between ST and same-priority interference, we must incorporate two additional cases: (i) when an ST frame preempts a higher-priority frame, and (ii) when an ST frame preempts a lower-priority frame. However, The ST preemption of the frame under analysis and the case with no preemption have already been discarded as worst-case scenario candidates in Lemma 1, thus they will not be analyzed again.

To prove Lemma 2, we will refer to the example in Fig. 5, where we analyze the three new candidates of maximum interference due to preemption: (a) same-priority preemption by an ST frame, (b) lower-priority preemption by an ST frame, and (c) high-priority preemption by an ST frame. These figures illustrate the worst-case response time of an AVB Class B frame m_i under the three scenarios. In this example, the frame under analysis m_i with C_i = 4 tu is interfered with by another same-priority frame with the same frame size (C = 4 tu) and an ST frame with C = 5 tu, taking into account the guard band and frame size. Also, we will consider one higher-priority queue (AVB Class A), and we will assume that there are constantly higher- and lower-priority frames queued for transmission in the output port, with a maximum frame size of C = 4 tu in both cases. Moreover, for simplicity, the credit slopes of both AVB Classes ($\alpha^+_{P_A,l}$, $\alpha^-_{P_A,l}$, $\alpha^+_{P_B,l}$, and $\alpha^-_{P_B,l}$) are assigned a value of 0.5, and the header is assigned a value of 1 tu.

According to the eligible interval approach, non-ST interference is constrained by the maximum achievable credit of the AVB Class of the frame under analysis, which can be calculated through Eqs. (6) and (7). Eq.(6) further categorizes the contributions into two parts: one dependent on the lower-priority interference, $LPI^l_i = C^{max}_{\mathbb{L},l} \times \left(1 + \frac{\alpha^+_{\mathbb{H},l}}{\alpha^-_{\mathbb{H},l}}\right)$, and another one corresponding to the higher-priority interference, $HPI^l_i = \frac{CR^{min}_{\mathbb{H},l}}{\alpha^-_{\mathbb{H},l}}$. Since $W^l_{c[k]}(t)$ does not affect the credit, it does not affect the maximum achievable P_i credit. However, the extra headers $V^l_{c[k]}(t)$ can affect the maximum achievable credit. In cases where ST preemption affects same-priority traffic, as shown in Fig. 5(a), the extra headers do not affect the maximum credit, as the cumulative credit over the same-priority interference is zero, as demonstrated in Lemma 1. Conversely, if the largest lower-priority frame ($C^{max}_{\mathbb{L},l}$) is preempted, as shown in Fig. 5(b), its size is increased by $V^l_{c[k]}(t)$. According to the eligible interval analysis, in the worst-case scenario, all credit accumulated due to $C^{max}_{\mathbb{L},l}$ in the highest

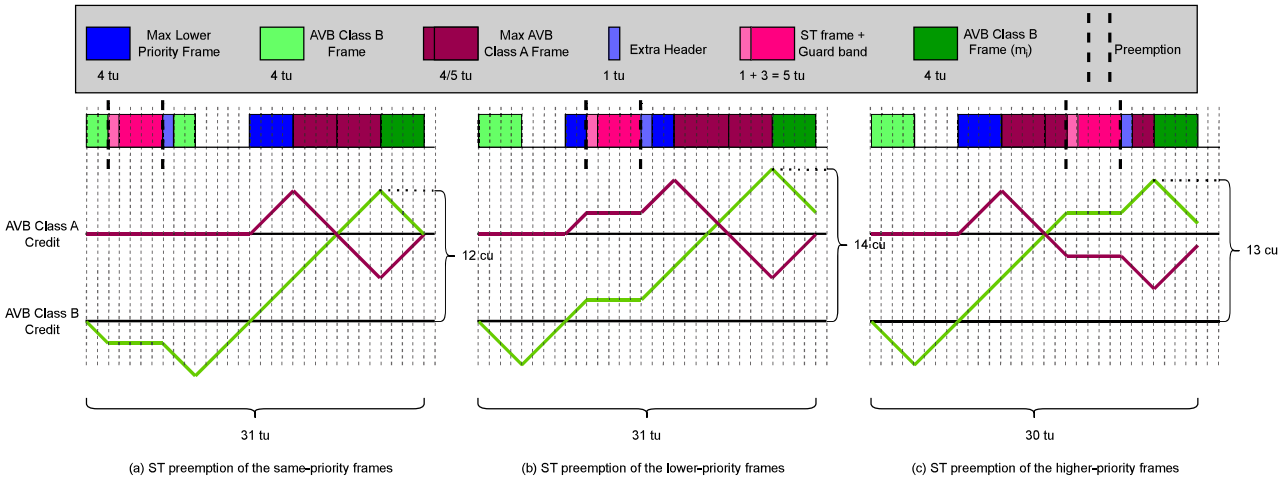

Fig. 5. Example of worst-case ST preemption with lower and higher priority traffic interference.

priority AVB classes, i.e. $C^{max}_{\mathbb{L},l} \times \alpha^{+}_{\mathbb{H},l}$, will be consumed by higher-priority classes before higher-priority interference starts. This implies that if frame $C^{max}_{\mathbb{L},l}$ is preempted by ST, its duration will be increased by $V^{l}_{c[k]}(t)$, resulting in an additional delay experienced by frame m_i equal to $V^{l}_{c[k]}(t) \times \left(1 + \frac{\alpha^{+}_{\mathbb{H},l}}{\alpha^{-}_{\mathbb{H},l}}\right)$.

Lastly, preempting the higher-priority frames does not produce the worst-case scenario. The higher-priority interference contribution, according to the eligible interval analysis and Eqs. (6) and (7), involves a summation of $C^{max}_{H_i,l} \times \frac{\alpha^{-}_{H_j,l}}{\alpha^{-}_{\mathbb{H},l}}$, where $\frac{\alpha^{-}_{H_j,l}}{\alpha^{-}_{\mathbb{H},l}}$ is always less than or equal to 1. If ST preempts a higher-priority frame, it implies an increase in $C^{max}_{H_i,l}$ by $V^{l}_{c[k]}(t)$, leading to its contribution to the delay being $V^{l}_{c[k]}(t) \times \frac{\alpha^{-}_{H_j,l}}{\alpha^{-}_{\mathbb{H},l}} \leq V^{l}_{c[k]}(t)$. Considering that $\left(1 + \frac{\alpha^{-}_{P_i,l}}{\alpha^{+}_{P_i,l}}\right)$ corresponding to ST preemption of same-priority frames and $\left(1 + \frac{\alpha^{+}_{\mathbb{H},l}}{\alpha^{-}_{\mathbb{H},l}}\right)$ corresponding to ST preemption of lower-priority frames are always greater than 1, ST preemption of higher-priority frames does not produce the WCRT. In conclusion, the WCRT of frame m_i occurs either when ST preempts the same-priority traffic, increasing the delay by $V^{l}_{c[k]}(t) \times \left(1 + \frac{\alpha^{-}_{P_i,l}}{\alpha^{+}_{P_i,l}}\right)$, or when ST preempts the largest lowest-priority frame, increasing the delay by $V^{l}_{c[k]}(t) \times \left(1 + \frac{\alpha^{+}_{\mathbb{H},l}}{\alpha^{-}_{\mathbb{H},l}}\right)$, depending on which preemption leads to the biggest delay, i.e. depending on $\max\left(\frac{\alpha^{-}_{P_i,l}}{\alpha^{+}_{P_i,l}}, \frac{\alpha^{+}_{\mathbb{H},l}}{\alpha^{-}_{\mathbb{H},l}}\right)$. Therefore, we obtain $V^{l}_{c[k]}(t) \times \left(1 + \max\left(\frac{\alpha^{-}_{P_i,l}}{\alpha^{+}_{P_i,l}}, \frac{\alpha^{+}_{\mathbb{H},l}}{\alpha^{-}_{\mathbb{H},l}}\right)\right)$.

Finally, recall that to obtain the WCRT of m_i in link l it is necessary to select the largest response time among all critical instant candidates through Eq. (17) where $STRT_i$ for link l and critical instant candidate $I^{l}_{c}[k]$ is calculated by Eq. (20).

D. Multi-hop Calculation

Finally, since the analysis is compositional in the sense that a frame passing through every hop is buffered, we sum the $STWCRT^{l}_{i}$ of each link in the path from the source to the destination of the frame under analysis m_i and add the ϵ factor for each traversed switch. This factor represents the delay suffered by the frame from being received at the input port of the switch to being enqueued in the TSN queue at the output port. The WCRT for frame m_i is calculated in Eq. (21)

$$WCRT_i = \sum_{l=1,\ldots,|\mathcal{L}_i|} STWCRT^{l}_{i} + (|\mathcal{L}_i| - 1) \times \epsilon \tag{21}$$

where, $STWCRT^{l}_{i}$ is determined by Eq. (17), which relies on the calculation of $STRT^{l}_{i,c[k]}$ by Eq. (20). Finally, $W^{l}_{c[k]}(t)$, $V^{l}_{c[k]}(t)$, HPI^{l}_{i}, LPI^{l}_{i}, and SPI^{l}_{i} are computed using Eqs. (13), (14), (3), (6), (7), respectively. The compositional structure of the WCRTA allows for its application even when certain delay sources are absent (i.e., their contribution is zero). Therefore, by considering all potential sources of delay, the WCRT can be accurately determined. However, note that each contribution in the formula is not independent. For instance, when quantifying ST interference, the interaction with other traffic types is considered, including the effect of extra headers on credit consumption or accumulation. Consequently, each component in the equations (STI, HPI, SPI, and LPI) accounts not only for the contribution of the specific traffic type (e.g., ST traffic) but also for the cumulative effect of all types of interference as a result of the interactions of that type of traffic with them.

VII. Experimental Setup

This paper uses an Evaluation Toolset (ETS) to evaluate the proposed WCRTA. The ETS comprises a comprehensive suite of integrated tools tailored for conducting automated experiments focused on the scheduling and schedulability analysis of TSN networks. This section explains the used ETS, including the modifications made specifically for this paper.

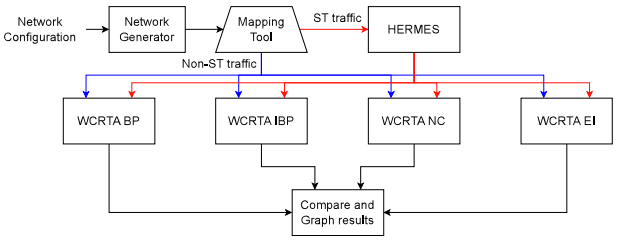

Fig. 6. Evaluation Toolset configuration.

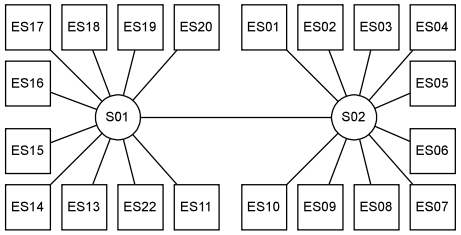

Fig. 7. Experimental network topology N1.

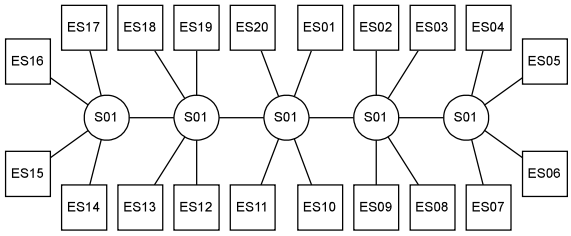

Fig. 8. Experimental network topology N2.

The configuration of the ETS used for this study is shown in Fig. 6. The input for the ETS consists of the network's configuration, involving its topology and traffic characteristics.

We consider two network topologies, as shown in Figs. 7 and 8, following a line-star topology. This topology is adequate for the analysis, as the only missing element that could impact the results is the presence of loops. However, since some of the compared WCRTAs do not support circular dependencies, this element has been excluded to ensure a fair comparison. Network N1 consists of a compact network with 2 switches, each with 10 end-stations, while network N2 presents a larger network with 5 switches and 4 end-stations connected to each switch. These network topologies are the input to the ETS.

To maintain manageable experiment durations, the network bandwidth was set to 100Mbps. This choice also ensures that the maximum allowed 100 frames can consistently reach the target utilization in almost every link. The frame length was selected from the range [500,1500] Bytes. Minimum and maximum allowed periods were set at 2000μs and 10000μs, respectively. Note that the number of frames generated can vary depending on the maximum allowed utilization of the links. For example, running an experiment that limits link utilization to 10% of the bandwidth will generate fewer frames than running an experiment that allows up to 90%.

The ETS starts with the Network Generator generating random traffic based on the topology and the traffic characteristics used as input. We enforced the distribution of 25% of the traffic being ST and 75% being AVB Class A and AVB Class B. For the experiments, the BE class and lower AVB priorities than class B were omitted due to limitations in the compared WCRTAs. We also evaluate the performance of the compared WCRTAs across various network utilizations, ranging from 5% to 60% for the small network and from 5% to 45% for the large network. We conducted 100 traffic generations for each utilization, making 2100 experiments. Each experiment involved analyzing up to 100 frames, resulting in the analysis of almost 210,000 frames.

The generated traffic is mapped into the different TSN traffic classes (ST, AVB Class A, and AVB Class B) in the next step, i.e., in the Mapping Tool (Fig. 6). The ST traffic will be scheduled using an existing heuristic algorithm [16]. Note that any other scheduling algorithm for ST traffic can be utilized, and a recent survey [20] identified their various features and characteristics. We selected a heuristic algorithm as it provides a good trade-off between fast and feasible results.

The AVB traffic and the ST schedule are used as input for each of the compared WCRTAs. In Fig. 6, WCRTA Busy Period (BP) and WCRTA Improved Busy Period (IBP) are the WCRTA based on busy period analysis [5], before and after removing the optimism introduced in Lemmas 1 and 2, respectively. WCRTA Network Calculus (NC) corresponds to the WCRTA implemented in Network Calculus [6], while WCRTA Eligible Interval (EI) represents the analysis proposed in this paper, i.e., the WCRTA based on the eligible interval extended with the new ST interference calculation and multi-hop behaviors. All WCRTAs were configured with both AVB Classes' credit slopes ($\alpha^{+}_{P_A,l}$, $\alpha^{-}_{P_A,l}$, $\alpha^{+}_{P_B,l}$, and $\alpha^{-}_{P_B,l}$) set to 0.5, which divides the available bandwidth equally between AVB Classes A and B corresponding to the experimental setup distribution of the AVB traffic. Additionally, a switch traversal factor ϵ of 0 was used for a fairer comparison since some analyses do not consider this factor.

Finally, the WCRTAs are compared using two methods. First, the schedulability of each WCRTA is determined for each bandwidth utilization. This comparison consists of calculating the percentage of generated networks that meet their time requirements according to each WCRTA. Second, the pessimism ratio between each previous WCRTA and the one proposed in this paper is calculated for each bandwidth utilization. Specifically, for each AVB-generated frame m_i, the pessimism ratio of WCRTA X to WCRTA EI is computed as follows.

$$\textit{Pessimism Ratio}_i = \frac{WCRTX_i}{WCRTEI_i} \tag{22}$$

This value illustrates how much pessimism is reduced by our proposed analysis (WCRTA EI) compared to the analysis named by X (BP, IBP, NC). Using this ratio, a pessimism ratio below 1 shows how much the proposed WCRTA is pessimistic compared to the previous analysis. Whereas, the ratio above 1 shows how much the proposed analysis in this paper performs better with respect to reducing pessimism compared to the

existing WCRTA.

Due to the random traffic generation and the extensive number of experiments conducted, we can confidently assert that these experiments do not bias any specific WCRTA. Therefore, the results accurately reflect the performance differences among the compared WCRTAs.

VIII. Results

This section presents the outcomes derived from the experiments outlined in Section VII. We assess the schedulability of the networks in relation to the bandwidth utilization percentage. To this end, we compare the additional pessimism introduced by the existing WCRTAs (WCRTA BP, IBP, and NC) in relation to the WCRTA EI proposed in this work.

A. Schedulability Comparison

Figs. 9 and 10 depict the percentage of schedulability achieved by each evaluated WCRTA with respect to the bandwidth utilization for N1 and N2, respectively. Note that the results for WCRTA BP and IBP overlap on the graph.

These graphs illustrate how the WCRTA introduced in this study consistently outperforms all prior WCRTAs in terms of schedulability despite the optimism present in one of them. The proposed WCRTA EI exhibits up to 90% higher schedulability compared to the WCRTAs BP and IBP based on busy periods with and without optimism and up to 25% higher schedulability at certain utilization levels, when compared to the WCRTA NC based on the Network Calculus model. Additionally, it is noteworthy that, despite the reduction in network schedulability with an increase in network hops (Fig. 10), the proposed WCRTA EI still demonstrates better performance than the previous solutions in terms of schedulability. All WCRTAs show zero schedulability after 25% network utilization for N1 and after 15% network utilization for N2. This is due to the accumulation of delays over multiple hops, a source of pessimism that is not in the scope of this work.

B. Additional Pessimism Comparison

In this subsection, we examine the WCRTs of only schedulable configurations as the analysis is deadline-constrained, i.e., the WCRT exceeding the deadline may not be correct.

Fig. 11 illustrates the pessimism ratio between the WCRTs of the AVB Class A traffic provided by WCRTA BP and IBP compared to WCRTA EI on networks N1 and N2. As can be seen, WCRTA BP shows better results (pessimism ratio lower than 1) compared to WCRTA EI. This is due to the optimism we identified in WCRTA BP, which shows an incorrect WCRT for class A traffic. After solving the optimism, shown as WCRTA IBP, both WCRTA IBP and WCRTA EI have identical values for WCRT of class A traffic. The figure shows how much optimism existed in the analysis based on the busy period [5] for class A traffic.

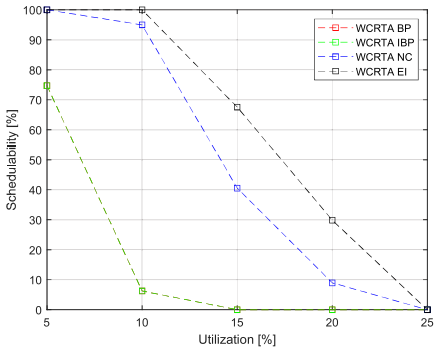

Fig. 9. Schedulability of the WCRTAs in network N1.

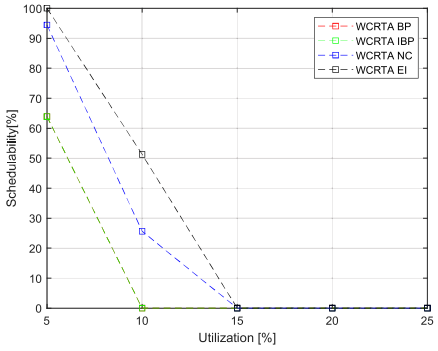

Fig. 10. Schedulability of the WCRTAs in network N2.

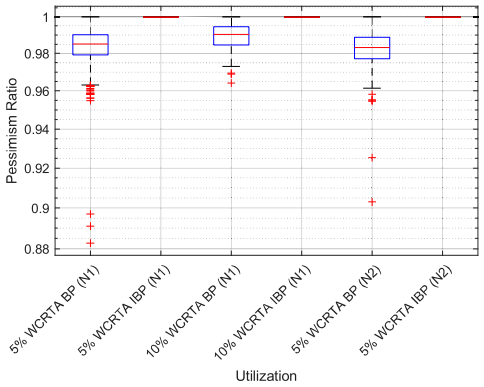

Fig. 11. Pessimism Ratio of the AVB Class A traffic of WCRTA BP and IBP in the networks N1 and N2.

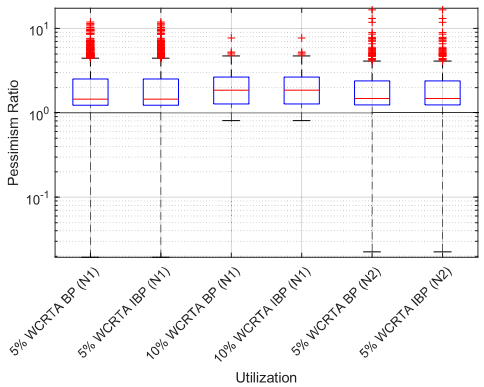

Fig. 12. Pessimism Ratio of the AVB Class B traffic of WCRTA BP and IBP in networks N1 and N2.

On the other hand, Fig. 12 depicts the pessimism ratio of AVB Class B traffic between WCRTAs BP and IBP compared to WCRTA EI for networks N1 and N2. As anticipated, despite WCRTA BP exhibiting optimistic ST interference, the pessimism associated with WCRTAs BP and IBP for AVB Class B traffic far surpasses that of WCRTA EI, potentially resulting in WCRTs tenfold higher. This discrepancy explains to a large extent the low schedulability of WCRTAs BP and IBP shown in Figs. 9 and 10.

Figs. 13 and 14 illustrate the pessimism ratio between the WCRTs of AVB Class A traffic provided by WCRTA NC compared to WCRTA EI on networks N1 and N2, respectively. These figures demonstrate that WCRTA NC yields WCRTs around 1.1 times larger than those achieved through WCRTA EI, resulting in an additional pessimism of approximately 10-15%.

Similarly, Figs. 15 and 16 show the pessimism ratio of AVB Class B traffic provided by WCRTA NC compared to WCRTA EI for networks N1 and N2, respectively. The results show an additional pessimism of around 10-15%, depending on the network size. The higher WCRT values provided by WCRTA NC account for its lower schedulability compared to WCRTA EI in Figs. 9 and 10.

Finally, upon comparing the outcomes of WCRTAs BP and IBP with those of WCRTA NC, it becomes evident that the latter exhibits higher schedulability. This is primarily attributed to the fact that, while WCRTA BP and IBP display lower pessimism in the WCRT of AVB Class A traffic, the considerably higher pessimism in the WCRT of AVB Class B traffic significantly hampers their effectiveness.

IX. Conclusion

For the successful adoption of Time-Sensitive Networking (TSN) in industry, developing an increasingly accurate and less pessimistic Worst-Case Response Time Analysis (WCRTA) is crucial. In this paper, we thoroughly reviewed existing WCRTAs, evaluating their strengths, weaknesses, and potential errors. Based on this examination, we introduced a novel WCRTA, for Audio-Video Bridging (AVB) traffic, that eliminates the optimism found in some prior works and yields less pessimistic results compared to the existing counterparts. Notably, our WCRTA demonstrated a reduction of around 15% in pessimism compared to the WCRTA based on the Network Calculus model [6] and around 100% improvement compared to the WCRTA based on busy period analysis [5]. The results provide strong evidence that our proposed WCRTA offers a better solution for meeting TSN's time requirements.

Acknowledgements

This research is supported by the Swedish Knowledge Foundation (KKS) under SEINE project, and the Swedish Govermental Agency for Innovation Systems (VINNOVA) under the FLEXATION and iSecure projects. Julian Proenza was supported by Grant pid2021-124348ob-i00, funded by MCIN/AEI/ 10.13039/501100011033 / ERDF, EU.

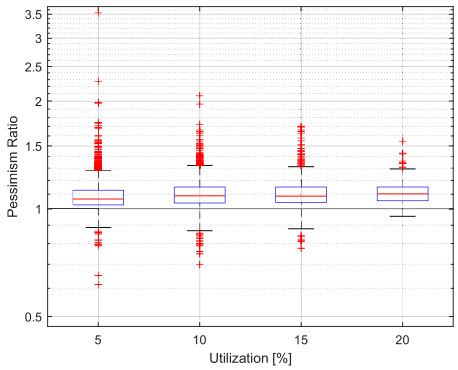

Fig. 13. Pessimism Ratio of the AVB Class A traffic of WCRTA NC in network N1.

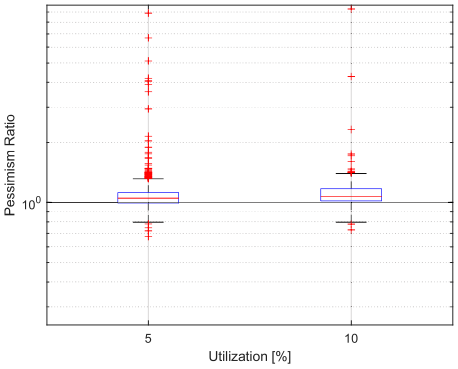

Fig. 14. Pessimism Ratio of the AVB Class A traffic of WCRTA NC in network N2.

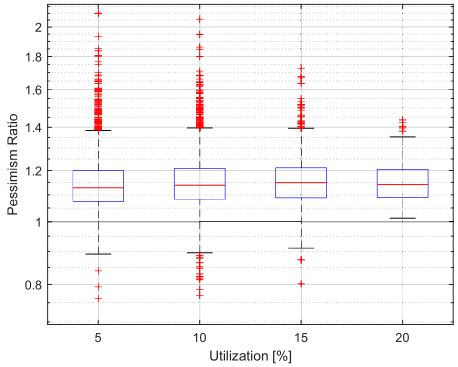

Fig. 15. Pessimism Ratio of the AVB Class B traffic of WCRTA NC in network N1.

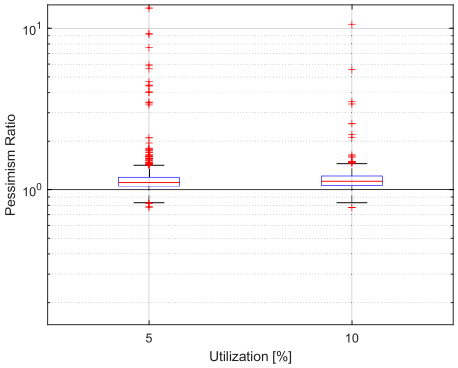

Fig. 16. Pessimism Ratio of the AVB Class B traffic of WCRTA NC in network N2.

REFERENCES

[1] J. Zhang, L. Chen, T. Wang, and X. Wang, "Analysis of tsn for industrial automation based on network calculus," in *2019 24th IEEE International Conference on Emerging Technologies and Factory Automation (ETFA)*, 2019, pp. 240–247.

[2] L. Lo Bello, G. Patti, and G. Vasta, "Assessments of real-time communications over TSN automotive networks," *Electronics*, vol. 10, no. 5, p. 556, 2021.

[3] Jover, Mateu and Barranco, Manuel and Proenza, Julián, "Opportunities and Specific Plans for Migrating from PRP to TSN in Substation Automation Systems," in *2023 IEEE 28th International Conference on Emerging Technologies and Factory Automation (ETFA)*, 2023, pp. 1–4.

[4] M. A. Ojewale, P. M. Yomsi, and B. Nikolić, "Worst-case traversal time analysis of tsn with multi-level preemption," *Journal of Systems Architecture*, vol. 116, p. 102079, 2021.

[5] L. Lo Bello, M. Ashjaei, G. Patti, and M. Behnam, "Schedulability analysis of Time-Sensitive Networks with scheduled traffic and preemption support," *Journal of Parallel and Distributed Computing*, vol. 144, pp. 153–171, 2020.

[6] L. Zhao, P. Pop, Z. Zheng, H. Daigmorte, and M. Boyer, "Latency analysis of multiple classes of AVB traffic in TSN with standard credit behavior using network calculus," *IEEE Transactions on Industrial Electronics*, vol. 68, no. 10, pp. 10 291–10 302, 2020.

[7] Cao, Jingyue and Cuijpers, Pieter JL and Bril, Reinder J and Lukkien, Johan J, "Tight worst-case response-time analysis for ethernet AVB using eligible intervals," in *2016 IEEE World Conference on Factory Communication Systems (WFCS)*. IEEE, 2016, pp. 1–8.

[8] ——, "Independent yet tight WCRT analysis for individual priority classes in ethernet AVB," in *Proceedings of the 24th International Conference on Real-Time Networks and Systems*, 2016, pp. 55–64.

[9] ——, "Independent WCRT analysis for individual priority classes in Ethernet AVB," *Real-Time Systems*, vol. 54, pp. 861–911, 2018.

[10] Maxim, Dorin and Song, Ye-Qiong, "Delay analysis of AVB traffic in time-sensitive networks (TSN)," in *Proceedings of the 25th International Conference on Real-Time Networks and Systems*, 2017, pp. 18–27.

[11] J. Diemer, J. Rox, and R. Ernst, "Modeling of Ethernet AVB networks for worst-case timing analysis," *IFAC Proceedings Volumes*, vol. 45, no. 2, pp. 848–853, 2012.

[12] J. Diemer, D. Thiele, and R. Ernst, "Formal worst-case timing analysis of Ethernet topologies with strict-priority and AVB switching," in *7th IEEE International Symposium on Industrial Embedded Systems (SIES'12)*. IEEE, 2012, pp. 1–10.

[13] L. Zhao, P. Pop, Z. Zheng, and Q. Li, "Timing analysis of AVB traffic in TSN networks using network calculus," in *2018 IEEE Real-Time and Embedded Technology and Applications Symposium (RTAS)*. IEEE, 2018, pp. 25–36.

[14] M. Seliem, A. Zahran, and D. Pesch, "Delay analysis of TSN based industrial networks with preemptive traffic using network calculus," in *2023 IFIP Networking Conference (IFIP Networking)*. IEEE, 2023, pp. 1–9.

[15] U. D. Bordoloi, A. Aminifar, P. Eles, and Z. Peng, "Schedulability analysis of Ethernet AVB switches," in *2014 IEEE 20th International Conference on Embedded and Real-Time Computing Systems and Applications*. IEEE, 2014, pp. 1–10.

[16] Bujosa, Daniel and Ashjaei, Mohammad and Papadopoulos, Alessandro V and Nolte, Thomas and Proenza, Julián, "HERMES: Heuristic multi-queue scheduler for TSN time-triggered traffic with zero reception jitter capabilities," in *Proceedings of the 30th International Conference on Real-Time Networks and Systems*, 2022, pp. 70–80.

[17] R. I. Davis, S. Kollmann, V. Pollex, and F. Slomka, "Controller Area Network (CAN) Schedulability Analysis with FIFO Queues," in *2011 23rd Euromicro Conference on Real-Time Systems*. IEEE, 2011, pp. 45–56.

[18] J. Maki-Turja and M. Nolin, "Fast and tight response-times for tasks with offsets," in *17th Euromicro Conference on Real-Time Systems (ECRTS'05)*, 2005.

[19] H. Daigmorte, M. Boyer, and L. Zhao, "Modelling in network calculus a TSN architecture mixing Time-Triggered, Credit Based Shaper and Best-Effort queues," 2018.

[20] C. Xue, T. Zhang, Y. Zhou, and S. Han, "Real-time scheduling for time-sensitive networking: A systematic review and experimental study," 2023.